

Published in final edited form as:

JAm Chem Soc. 2011 March 30; 133(12): 4398–4403. doi:10.1021/ja108209w.

# Kinetic Isotope Effects of L-Dopa Decarboxylase

#### Yen-lin Lin and Jiali Gao

Department of Chemistry, Digital Technology Center and Supercomputing Institute University of Minnesota, Minneapolis, MN 55455

### **Abstract**

A mixed centroid path integral and free energy perturbation method (PI-FEP/UM) has been used to investigate the primary carbon and secondary hydrogen kinetic isotope effects (KIEs) in the amino acid decarboxylation of L-Dopa catalyzed by the enzyme L-Dopa decarboxylase (DDC) along with the corresponding uncatalyzed reaction in water. DDC is a pyridoxal 5'-phosphate (PLP) dependent enzyme, which undergoes an internal proton transfer between the zwitterionic protonated Schiff base configuration and the neutral hydroxyimine tautomer. It was found that the cofactor PLP makes significant contributions to lowering the decarboxylation barrier, while the enzyme active site provides further stabilization of the transition state. Interestingly, the O-protonated configuration is preferred both in the Michaelis complex and at the decarboxylation transition state. The computed kinetic isotope effects (KIE) on the carboxylate C-13 are consistent with that observed on decarboxylation reactions of other PLP-dependent enzymes, whereas the KIEs on the alpha carbon and secondary proton, which can easily be validated experimentally, may be used as a possible identification for the active form of the PLP tautomer in the active site of DDC.

# Introduction

Pyridoxal 5'-phosphate (PLP) facilitates a wide range of chemical transformations in enzymes. 1-2 Although common features of PLP-dependent enzymes such as transamination and stabilization of the external aldimine have been well characterized, 1,3 the critical role of the internal proton transfer on catalysis remains poorly understood. The most comprehensive studies of this process were conducted by Toney, Limbach and their coworkers on a series of model Schiff bases in solution and in solid state. S-8 Spectroscopic results on PLP-dependent decarboxylases provided additional insight. In this article, we report a theoretical study of the primary (1°) 13C and secondary (2°) H kinetic isotope effects (KIEs) on the decarboxylation of L-dopa catalyzed by the PLP-dependent enzyme L-dopa decarboxylase (DDC) with the cofactor both in the zwitterionic N-protonated Schiff base (PBS) and the neutral O-protonated hydroxyimine (HI) form (Scheme 1). The present work provides an understanding of the role of the internal proton transfer between the Schiff base and the hydroxyl group of PLP on the transition state of the enzymatic reaction. Furthermore, we make a theoretical prediction to identify the active form of the PLP tautomer in the active site of DDC based on the decarboxylation KIEs.

The external aldimine between PLP and an amino acid substrate consists of three titratable sites in addition to the phosphate group, <sup>8,15</sup> including the pyridine nitrogen, the 3-oxo oxygen and the imine nitrogen of the Schiff base linkage; the specific protonation state and

gao@jialigao.org.

site are critical to catalysis. Under physiological conditions, the external aldimine would retain only one proton, whereas the protonation of the pyridine nitrogen site is strongly dependent on the amino acid, with which it forms a specific hydrogen bond in the active site. In the enzyme L-dopa decarboxylase, <sup>12</sup> the carboxylate side chain of Asp271 accepts a hydrogen bond from the protonated pyridinium ion of PLP. Richard and coworkers suggested that PLP-dependent enzymes select the zwitterionic external aldimine complex, in which pronation at the imine nitrogen is preferred.  $^{1,16}$  Consequently, the  $\alpha$ -carbon acidity has a relatively high pKa of 17 as a result of carbanion stabilization. <sup>17–19</sup> The proton that forms an internal hydrogen bond between the 3-oxo anion and the imine nitrogen of the external aldimine can undergo proton transfer from the N-protonated Schiff base to the Oprotonated hydroxyimine, formally corresponding to a tautomerization (Scheme 1). Toney and Limbach and their coworkers demonstrated that the intramolecular proton transfer is coupled to the protonation state of the pyridine ring, which favors the N-protonated PSB in solid state and in polar aprotic solvent when it is protonated.<sup>6,8</sup> However, there is no coupling in aqueous solution due to competition between intramolecular and intermolecular hydrogen bonds.<sup>5,7</sup>

Dopa decarboxylase catalyzes the conversion of L-dopa into dopamine in the treatment of Parkinson's disease, which has been extensive studied, providing a wealth of kinetic data for validation of our theoretical model. 9-10 Crystal structures of the PLP-enzyme binary complex and a inhibitor ternary complex have been determined. 12 We have previously investigated the internal proton transfer of PLP and the relative stability of the zwitterionic N-protonated (PSB) and the neutral O-protonated (HI) isomers in water and in DDC using a combined quantum mechanical and molecular mechanical (QM/MM) method.<sup>4</sup> It was found that the zwitterionic PSB configuration is more stable in the gas phase, whereas the neutral form HI is slightly preferred by about 1 kcal/mol in aqueous solution and in the active site of the enzyme. The latter is somewhat surprising in that the protonated Schiff base is generally thought to be preferred in catalysis because it provides a key stabilization of the αcarbanion, responsible for the exceptionally high acidity of a carbon acid and critical to amino acid racemization and transamination reactions. In both types of reactions, the removal of a proton at the α-carbon of the external aldimine substrate results in a net gain of one negative charge on the ligand, which can be effectively stabilized by a neighboring cation and further delocalized into the pyridinium ring, a so-called electron sink.<sup>2–3</sup> However, the total charge of the external aldimine is unchanged in the active site during PLP-dependent decarboxylation reactions, and the strong electrostatic interactions between the carboxylate anion of the substrate and the PSB in fact has an inhibition effect to the removal of carbon dioxide. Thus, the neutral form of the Schiff base and a hydroxyl isomer of the external aldimine could be preferred for enzymatic decarboxylation processes.

In the present study, we aim to understand the effect of the intramolecular proton transfer of the external aldimine on the decarboxylation mechanism in L-dopa decarboxylase. We employ a combined QM/MM and path integral approach, in which both the potential energy surface (PES)<sup>20–21</sup> for the chemical process and the nuclear quantum effects (NQEs)<sup>22–23</sup> are treated quantum-mechanically, to determine the kinetic isotope effects associated with the decarboxylation reaction both in water and in the DDC enzyme. A novel centroid path integral (PI) method (PI-FEP/UM) that couples umbrella sampling for determination of the potential of mean force (PMF) and free energy perturbation theory between heavy and light isotopes to compute KIEs is used.<sup>22–27</sup> The computational results show that the reaction free energy profiles for the L-dopa decarboxylation reaction exhibit characteristic features in the PSB and the HI form of the substrate, which are reflected in the computed KIEs. In the following, we present the computational details, followed by results and discussion. The main findings are summarized in the conclusion.

# **Computational Details**

# Model for the External PLP Schiff base and Dopa Decarboxylase

The X-ray crystal structure of pig kidney DDC in a ternary complex with the PLP cofactor and carbiDopa inhibitor (PDB entry: 1JS3)<sup>12</sup> was used to generate the initial Michaelis complex structure containing the PLPL-dopa external Schiff base. DDC is a homodimer, consisting of 486 amino acid residues in each subunit. There is only one active site and one PLP cofactor per dimer structure, located at the interface of the two monomers. In the active site, the crystal structure reveals that there is strong interaction between the pyridine nitrogen and the side chain of Asp271, a typical structural feature in PLP-dependent enzymes.<sup>2</sup> Given that the pKa of the pyridine of the external aldimine is somewhat more basic than a carboxylate group, <sup>1</sup> we have kept the pyridine nitrogen of the dopa-external aldimine protonated, (PLP(H+)~L-dopa), throughout the simulation. The residues in the missing loop (residue 328′–339′) were modeled as described in ref. 4. The active site residue Lys303, which is released from the internal aldimine Schiff base, was set neutral, ready for the next reaction cycle. His192, His262, His348, His386, and His434 that form ion-pairs or are exposed to the solvent were protonated, and we treated the remaining titratable residues corresponding to ionization states at pH 7.

### **Potential Energy Function**

The decarboxylation reaction of the external aldimine substrate PLP(H+)~L-dopa was modeled by using a combined quantum QM/MM potential. <sup>20–21,28</sup> The boundary between QM and MM regions is located at the C5A position (Scheme 2), which is described by the generalized hybrid orbital (GHO) method. <sup>29–30</sup> A total of 39 atoms are included in the QM region and the Austin Model 1 (AM1)<sup>31</sup> semiempirical Hamiltonian was used. Previous studies of several decarboxylation reactions, including the decarboxylation of 3-Carboxybenzisoxazole in Water, <sup>32</sup> orotidine 5'-monophosphate (OMP) in water and in OMP dcarboxylase, <sup>33–34</sup> biotin carboxylation by acetyl-CoA carboxylase, <sup>35</sup> N-methyl picolinate in water, <sup>25</sup> and the closely related L-ornithine by ornithine decarboxylase show that the AM1 model can yield good geometrical and energetic results for the decarboxylation reaction. In hybrid QM/MM simulations, The CHARMM22 all-atom force field <sup>37</sup> was used to represent the protein and the phosphate group of the PLP, whereas the three point charge TIP3P model <sup>38</sup> was used to describe water.

### **Molecular Dynamics Simulations**

Periodic boundary conditions along with the isothermal-isobaric (NPT) ensemble at 298.15 K and 1 atm were used. Long-range electrostatic interactions are modeled by using a QM/MM particle-mesh Ewald method,<sup>39</sup> whereas van der Waals interactions were feathered to zero between 12 Å and 13 Å with a shift function. All bonds involving hydrogen atoms, except those in the QM region, were constrained to their equilibrium distances using the SHAKE algorithm. The integration step in dynamics simulations was 1 fs.

The enzyme system was embedded in a cubic box of water molecules about  $93 \times 93 \times 93$  Å  $^3$ . The resulting system has a net charge of zero and no additional counterions were added. The final model of the enzyme system consists of 75514 atoms, including 20203 water molecules. The system has been thoroughly equilibrated during the study of the internal proton transfer process in DDC. For the external aldimime reactions in water, the center of mass of the solute was solvated at the center of a cubic water box with a box length of 45 Å. Two sodium ions (Na+) were added to neutralize the systems

A series of umbrella sampling simulations were performed to compute the potentials of mean force (PMFs) for the decarboxylation reactions of the PLP-L-dopa external aldimine

in the N-protonated and O-protonated configurations but in the enzyme dopa decarboxylase and in water without the catalyst. For each reaction, the reaction coordinate, as depicted in Figure 2, is defined as the distance between the carboxyl carbon (C) and the a-carbon ( $C_{\alpha}$ ) of the amino acid L-dopa:

$$RC \equiv R\left(C_{\alpha} - C^{CO_{-}}\right)$$

We used a total of 13 windows for the enzymatic reactions and 12 windows for the model reactions. For the enzymatic simulations, each window consisted of 30-ps equilibration, followed by additional 30 ps for averaging and trajectory collection. For the model reactions, each window was equilibrated for 50 ps and subsequently sampled for another 50 ps. The weighted histogram analysis method (WHAM)<sup>40</sup> was used to analyze the probability density and to obtain the free energy profiles for the unbiased systems along the proton transfer reaction coordinate.

### **Computation of Kinetic Isotope Effects**

The potential of mean force obtained from classical molecular dynamics simulations above, employing a combined QM/MM potential, does not include nuclear quantum effects (NQEs), which are required to compute kinetic isotope effects (KIEs). In the current work, we employ a coupled free energy perturbation and umbrella sampling simulation technique in Feynman centroid path integral calculations (PI-FEP/UM)<sup>22,27</sup> to describe the nuclear quantum effects. In the PI-FEP/UM calculation, the ratio of the quantum partition function for different isotopes, which yields the corresponding KIEs, is obtained by free energy perturbation from a light isotope mass into a heavier one within the same centroid path integral simulation. Consequently, the PIFEP/UM method can yield highly accurate results on computed KIEs through a single simulation rather than separate calculations for different isotopic reactions.<sup>23</sup> The PI-FEP/UM method has been demonstrated in a series of studies of chemical reactions in solution and in enzymes.<sup>18–19,22–27,41</sup>

In the centroid path integral simulation, we represent each quantized atom by a ring of particles or beads, whose geometrical center (centroid) is constrained to its classical position. 42–43 Thus, for each classical configuration sampled in molecular dynamics umbrella sampling simulations, we perform PI sampling to obtain the NOEs for nuclear motions.<sup>22,44-45</sup> When the PI calculations are performed along the reaction coordinate, we obtain a quantum mechanical correction at each point of the reaction coordinate, resulting in a QM-PMF as a function of the centroid reaction coordinate. The approach of NQE corrections to the classical configurations was used in computer simulations by Sprik et al., 44 and has been exploited in other works. 25,45 In the present study, we used 32 beads for each of the three isotopic sites for KIE calculations along with the atoms directly connected to them for the dopa decarboxylation reaction both in DDC and in water. Previous studies have shown that this treatment yields good convergence in the overall quantum corrections for a number of systems in water and in enzymes. 18-19,22-27,41 About 2,400 configurations were extracted from the MD trajectory. Ten separate centroid path integral simulations were carried out, each of which was sampled by 11 free particle distributions for equilibration and 50 PI configurations to estimate the KIEs. The final results are determined from the cumulated path integral samplings, while the standard errors (1 $\sigma$ ) are estimated using the ten separate averages. The results are listed in Tables S1 and S2.

There are two contributions from our work in the development of the PI-FEP/UM method,<sup>22</sup> which are distinctively different from previous works and the approach of Ref. 45. We extended and implemented a bisection sampling technique,<sup>24,46</sup> which greatly improves the

convergence of path integral calculations. Second and most importantly, we developed a free energy perturbation scheme for computing the ratio of the quantum partition functions of different isotopic reactions in one single simulation, which yields the kinetic isotope effects directly.<sup>22</sup> This approach avoids the essentially insurmountable difficulty in the direct approach<sup>45,47–48</sup> that takes the difference of two separate simulations, one for each isotopic reaction, whose statistical fluctuations are as large as or greater than the difference itself in KIE calculations. Although reasonable estimate can be obtained for primary H/D isotope effects, which are typically very large, it is very difficult to yield meaningful results for secondary or heavy atom primary KIEs using the direct approach. To our knowledge, secondary KIEs have not been reported from path integral simulations prior to the development of the PI-FEP/UM method, which has been implemented into and distributed with CHARMM.

#### **Results and Discussion**

### Transition state stabilization

The computed centroid potentials of mean force including nuclear quantum effects for the DDC-catalyzed and the corresponding uncatalyzed PLP-dopa external aldimine in water are shown in Figure 1. The free energy profiles are anchored to zero at the reactant state both for the N-protonated PSB and the O-protonated HI configurations for convenience of comparison. Note that we have previously estimated that the free energy difference is -1.3kcal/mol in favor of the Michaelis complex with the O-protonated PLP isomer, whereas the difference is -2.0 kcal/mol for the PLP-dopa external aldimine species in water.<sup>4</sup> In aqueous solution, the free energy barriers for the decarboxylation reaction of the PLP-dopa external aldimine complex are essentially the same both for the zwitterionic PSB and the neutral hydroxyimine tautomers, suggesting that there is no particular preference for the  $\alpha$ carbanion stabilization by a neighboring (N-protonated) iminium ion in the present decarboxylation reaction. This is due to the fact that the decarboxylation reaction retains the anion from the reactant state as a carbanion in the transition state, both of which are stabilized by the PSB. The enzyme lowers the free energy barrier by about 8 (6) kcal/mol with the PLP cofactor in the N-protonated PSB (O-protonated hydroxyimine) form; the computed barrier height is 17.3 kcal/mol including NQEs, which may be compared with the experimental value of 16.0 kcal/mol. 10 The decarboxylation of the external aldimine, in water in the absence of an enzyme, is known to be slow, which takes place at temperatures above 100 °C;<sup>49–50</sup> the barrier for the decarboxylation of the amino acid L-dopa itself is exceedingly high with a computational value of 42 kcal/mol in water. The latter is consistent with Wolfenden's experimental data on similar systems (41 kcal/mol).<sup>50</sup> The PLP cofactor itself provides a dominant contribution to the overall catalytic effects, 1 lowing the decarboxylation barrier by about 16 kcal/mol, whereas the enzyme further lowers the barrier by about 8 kcal/mol. The catalysis by the PLP cofactor can be attributed to the charge delocalization effect through the resonance of the pyridine-imine  $\pi$ -conjugation to the anion quinonoid intermediate. A similar feature has also been demonstrated in our studies of the alanine racemization reaction in alanine racemase. 18-19

A distinctive feature in Figure 1 is that the transition state is earlier for the O-protonated tautomer of the PLP cofactor than that for the N-protonated Schiff base, both in the enzymatic and in the uncatalyzed reactions. The average reaction coordinate, the distance  $C_{\alpha}$  – C, at the transition state is 2.07 Å for the O-protonated aldimine, and 2.17 Å for the N-protonated system in the active site. This is further reflected by the concomitant change in the O-C-O angle of the carboxyl group (Table 1), which is about 3° to 5° greater for the reaction with the N-protonated Schiff base configuration than that in the O-protonated tautomer. The intramolecular O3...H...N hydrogen bond in the reactant state (RS) and the transition state (TS) for the decarboxylation reaction in the N-protonated configuration of

the PLP has a shorter donor-acceptor distance than that in the O-protonated isomer of the cofactor since the former has stronger electrostatic interactions in the zwitterion pair. As a result, the internal torsion about the dihedral angle of  $N-C4A-C4-C3~(\chi)$  is restricted to be roughly coplanar with the pyridine ring with rather small fluctuations  $(\pm~3^{\circ}).$  On the other hand the average  $\chi$  is  $135\pm15^{\circ}$  at the TS when the PLP cofactor adopts the O-protonated configuration. In this case the PLP external aldimine favors intermolecular hydrogen bonds with residues Thr246 and Lys303. It is also important to notice the different roles of Thr246, which acts as a hydrogen bond donor to interact with the 3-oxo anion in the N-protonated PLP isomer, but it becomes an acceptor from the 3-hydroxy group of the external aldimine at an average distance of 2.40 Å in the O-protonated PLP configuration. For comparison, in aqueous solution, Limbach, Toney and coworkers found that the intramolecular hydrogen bond in PLP cofactor is not maintained in aqueous solution due to competition with the solvent.  $^7$ 

Figure 1 shows that the product region is more strongly stabilized for the reaction in the O-protonated configuration, whereas the free energy change in the product region is flat. This may be somewhat surprising since the iminium ion of the Schiff base linkage has been proposed to provide key stabilization of the  $\alpha$ -carbanion; however, the zwitterions of the PLP cofactor interferes with hydrogen bonding interactions with the solvent, and the neutral O-protonated PLP configuration favors stabilization of the carbanion from the decarboxylation reaction. We have not specifically addressed the reversibility of the carbon dioxide recombination reaction in the present work.

# **Kinetic Isotope Effects**

Computed 1° and 2° KIEs from PI-FEP/UM simulations are listed in Table 1 along with key geometrical results at the transition state. The carbon 1° KIEs range from 1.03 to 1.05 both for the enzyme and the uncatalyzed reactions in water. KIEs for the present DDC enzyme have not been measured, although carboxyl <sup>13</sup>C-KIEs are widely used to probe PLPdependent decarboxylations by analyzing the product CO<sub>2</sub>:51-52 the observed KIEs are in the range of 1.01 to 1.06, keeping in mind that these are not intrinsic effects of the decarboxylation step. In the closely related PLP-dependent L-ornithine decarboxylase, Swanson et al. found that the native substrate has an observed KIE of 1.0325, and it is increased to 1.0633 for the substrate L-Lys.<sup>52</sup> The latter value was considered to be close to the intrinsic KIE for the decarboxylaiton step as it becomes rate-limiting. In DDC catalysis, the reaction of the O-protonated isomer of the external aldimine, which has the lowest reaction barrier (Figure 1), has a computed carboxyl <sup>13</sup>C KIE of 1.053, whereas the Nprotonated form has a similar value of 1.047. The KIEs for the uncatalyzed reactions are also about 1.05. The range of the computed KIEs is in good accord with experiments on PLP-dependent enzymes, which provides a validation of the present PIFEP/UM method.<sup>51–52</sup>

The calculated carboxyl  $^{13}$ C-KIEs in Table 1 are closely related to the small, but significant, variations in the O-C-O bond angle of the carboxylate group. The average bond angles at the transition state are close to  $150^{\circ}$ , about mid-way from the reactant (about  $122^{\circ}$ ) to the product states ( $180^{\circ}$ ), consistent with the estimated Pauling bond order of about 0.4 for the  $C_{\alpha}$ -C bond. The transition state of the O-protonated tautomer in the active site has the smallest O-C-O bond angle of the four decarobxylation reactions, indicating an early transition state with the least gain in bond order on the  $CO_2$  group. On the other hand, the N-protonated isomer has the largest O-C-O angle, indicative of enhanced force constant in the  $CO_2$  stretch and a late transition state (mirrored by a larger value in the reaction coordinate). Thus, for the N-protonated configuration of the PLP cofactor in the enzymatic reaction, the reduction in the difference of zero-point energy (ZPE) (between  $^{12}C$  and  $^{13}C$ ) associated with the  $C_{\alpha}$ -C stretch is accompanied by an increase in the O-C-O stretching frequency,

orthogonal to the reaction coordinate, in going from the reactant to the transition state. The two compensating factors yield a smaller computed carboxyl KIE in the N-protonated PLP aldimine substrate. The change in O-C-O angle is less for the O-protonated configuration, resulting in a greater KIE at the carboxyl site of the substrate.

The rehybridization at the  $C_{\alpha}$  position from sp<sup>3</sup> to sp<sup>2</sup> along the decarboxylation path is best reflected by the  $2^{\circ} {}^{1}k/{}^{2}k$  (H<sub>0</sub>) KIEs (Table 1). Here, the primary  ${}^{12}k/{}^{13}k$  (C<sub>0</sub>) effects are much smaller than those at the carboxyl carbon, and they do not show significant dependence on the tautomerism of the cofactor. The deuteron  ${}^{1}k/{}^{2}k$  (H<sub>a</sub>) KIE is coupled both to the C-H stretching frequency and to the hydrogen "out-of-plane" bending mode about the  $C_{\alpha}$ =N  $\pi$ -plane that is being developed at the transition state. The former increases from about 2900 cm<sup>-1</sup> to 3100 cm<sup>-1</sup> in going from an sp<sup>3</sup> to an sp<sup>2</sup> carbon, whereas the latter changes from ca. 1300 cm<sup>-1</sup> for an sp<sup>3</sup> C-H deformation mode in the reactant state to about 800 cm<sup>-1</sup> in the product state. The development of the  $C_{\alpha}$ =N double bond character is indicated by the distance  $R(C_q = N)$  in Table 1. Consequently, a shorter  $C_q = N$  distance corresponds to greater sp<sup>2</sup> character and a larger force constant in the C-H stretch, but a smaller bending frequency. In the N-protonated configuration (a longer  $C_q$ =N bond distance at the transition state), the dominant factor is the change in the C-H deformation mode, giving rise to greater decrease in ZPE, thereby, relatively large secondary KIEs. We attribute the slow change in the  $C_{\alpha}$ =N double bond at the TS to the cationic Schiff base, hindering charge delocalization into the cationic pyridine. For the O-protonated isomer of the cofactor, a greater C<sub>0</sub>=N double bond character is developed, resulting in an increase in the C-H stretch at the transition state. Thus, the  $2^{\circ} {}^{1}k/{}^{2}k$  (H<sub>q</sub>) KIEs are relatively small and even inverse for the reaction in water (Table 1).

Is there a simple way to distinguish between the N-protonated and O-protonated tautomers of the PLP-dopa external aldimine in the DDC-catalyzed decarboxylation? The data in Table 1 suggest that the diagnostic feature distinguishing the two configurations is an examination of the overall trends of primary (<sup>13</sup>C) and secondary (<sup>2</sup>H) KIEs. For the N-protonated aldimine, the 2° KIE for the alpha hydrogen,  ${}^{1}k/{}^{2}k$  (H<sub>a</sub>), is 1.14, greater than 1.1, accompanied by a carboxyl C-13 intrinsic KIE in the middle range for similar reactions. On the other hand, for the O-protonated configuration,  ${}^{1}k/{}^{2}k(H_{a})$  is below 1.1 (1.05), and the primary carbon KIEs are found at the higher end. Previously, we have determined that the O-protonated form of the external aldimine is preferred over the N-protonated tautomer by 1.3 kcal/mol.<sup>4</sup> The present computed PMFs show that the free energy barrier is also lower by 1.5 kcal/mol for the reaction in the O-protonated hydroxyimine configuration than that in the N-protonated form. Interestingly, Sicinska et al. adopted the O-protonated aldimine in their study of the decarboxylation by L-ornithine decarboxylase. <sup>36</sup> These results conclude that the O-protonated hydroxyimine tautomer of the PLP-dopa external aldimine is preferred in the DDC-catalyzed decarboxylation, which exhibits a 2° deuteron KIE below 1.1 and a primary 13C KIE of greater 1.05 as a diagnostic indicator of the transition state.

# **Conclusions**

A mixed centroid path integral and free energy perturbation method (PI-FEP/UM) has been used to investigate the primary carbon and secondary hydrogen kinetic isotope effects (KIEs) in the amino acid decarboxylation of L-Dopa catalyzed by the enzyme L-Dopa decarboxylase (DDC) as well as the corresponding uncatalyzed reaction in water. DDC is a pyridoxal 5'-phosphate (PLP) dependent enzyme, which undergoes an intramolecular proton transfer between the N-protonated Schiff base and the 3-oxo anion. The specific protonation state is important to enzyme catalysis and the aim of the present study is to provide an understanding of effects of N- and O-protonation in the external aldimine cofactor on the decarboxylaiton reaction catalyzed by DDC. The present theoretical investigation revealed

that the O-protonated hydroximine form of the unprotonated Schiff base in the cofactor is the preferred configuration in catalysis by DDC. The computed KIEs are consistent with that observed on decarboxylation reactions of other PLP-dependent enzymes. Furthermore, the computational prediction of the kinetic isotope effects can be conveniently validate experimentally and used as a possible identification of the active form of the PLP tautomer in the active site of DDC based on the decarboxylation KIEs.

# **Supplementary Material**

Refer to Web version on PubMed Central for supplementary material.

# **Acknowledgments**

We thank Professor Dan Major and Dr. Alessandro Cembran for computational assistance, and Professor Michael Toney for discussion at the 2010 Gordon Conference on Isotope Effects, which led to the KIE calculations presented here. This work has been supported by the National Institutes of Health (grant no. GM46736).

### **REFERENCES**

- (1). Richard JP, Amyes TL, Crugeiras J, Rios A. Curr Opin Chem Biol. 2009; 13:475. [PubMed: 19640775]
- (2). Toney MD. Arch. Biochem. Biophys. 2005; 433:279. [PubMed: 15581583]
- (3). Frey, PA.; Hegeman, AD. Enzymatic Reaction Mechanisms. Oxford University; New York: 2007.
- (4). Lin YL, Gao J. Biochemistry. 2010; 49:84. [PubMed: 19938875]
- (5). Sharif S, Denisov GS, Toney MD, Limbach H-H. J. Am. Chem. Soc. 2006; 128:3375. [PubMed: 16522119]
- (6). Sharif S, Denisov GS, Toney MD, Limbach H-H. J. Am. Chem. Soc. 2007; 129:6313. [PubMed: 17455937]
- (7). Sharif S, Huot MC, Tolstoy PM, Toney MD, Jonsson KHM, Limbach H-H. J. Phys. Chem. B. 2007; 111:3869. [PubMed: 17388551]
- (8). Sharif S, Schagen D, Toney MD, Limbach H-H. J. Am. Chem. Soc. 2007; 129:4440. [PubMed: 17371021]
- (9). Hayashi H, Mizuguchi H, Kagamiyama H. Biochemistry. 1993; 32:812. [PubMed: 8422386]
- (10). Hayashi H, Tsukiyama F, Ishii S, Mizuguchi H, Kagamiyama H. Biochemistry. 1999; 38:15615. [PubMed: 10569946]
- (11). Nishino J, Hayashi H, Ishii S, Kagamiyama H. J. Biochem. (Tokyo). 1997; 121:604. [PubMed: 9133632]
- (12). Burkhard P, Dominici P, Borri-Voltattorni C, Jansonius JN, Malashkevich VN. Nature Struct. Biol. 2001; 8:963. [PubMed: 11685243]
- (13). Minelli A, Charteris AT, Voltattorni CB, John RA. Biochem J. 1979; 183:361. [PubMed: 534502]
- (14). Voltattorni CB, Minelli A, Vecchini P, Fiori A, Turano C. Eur J Biochem. 1979; 93:181. [PubMed: 436828]
- (15). Dixon JE, Bruice TC. Biochemistry. 1973; 12:4762. [PubMed: 4773854]
- (16). Richard JP, Amyes TL. Bioorg Chem. 2004; 32:354. [PubMed: 15381401]
- (17). Toth K, Richard JP. J. Am. Chem. Soc. 2007; 129:3013. [PubMed: 17298067]
- (18). Major DT, Nam K, Gao J. J. Am. Chem. Soc. 2006; 128:8114. [PubMed: 16787057]
- (19). Major DT, Gao J. J. Am. Chem. Soc. 2006; 128:16345. [PubMed: 17165790]
- (20). Gao J, Xia X. Science. 1992; 258:631. [PubMed: 1411573]
- (21). Gao J, Ma S, Major DT, Nam K, Pu J, Truhlar DG. Chem. Rev. 2006; 106:3188. [PubMed: 16895324]
- (22). Major DT, Gao J. J. Chem. Theory Comput. 2007; 3:949.
- (23). Gao J, Wong K-Y, Major DT. J. Comput. Chem. 2008; 29:514. [PubMed: 17722009]

- (24). Major DT, Gao J. J. Mol. Graph. Model. 2005; 24:121. [PubMed: 15936231]
- (25). Major DT, Garcia-Viloca M, Gao J. J. Chem. Theory Comput. 2006; 2:236.
- (26). Major DT, Heroux A, Orville AM, Valley MP, Fitzpatrick PF, Gao J. Proc. Natl. Acad. Sci. 2009
- (27). Gao, J.; Wong, K-Y.; Major, DT.; Cembran, A.; Song, L.; Lin, Y-L.; Fan, Y.; Ma, S. Quantum Tunnelling in Enzyme-Catalysed Reactions. Allemann, RK., editor. 2009. p. 105
- (28). Gao, J. Rev. Comput. Chem. Lipkowitz, KB.; Boyd, DB., editors. Vol. Vol. 7. VCH; New York: 1995. p. 119
- (29). Gao J, Amara P, Alhambra C, Field MJ. J. Phys. Chem. A. 1998; 102:4714.
- (30). Amara P, Field MJ, Alhambra C, Gao J. Theor. Chem. Acc. 2000; 104:336.
- (31). Dewar MJS, Zoebisch EG, Healy EF, Stewart JJP. J. Am. Chem. Soc. 1985; 107:3902.
- (32). Gao J. J. Am. Chem. Soc. 1995; 117:8600.
- (33). Wu N, Mo Y, Gao J, Pai EF. Proc. Natl. Acad. Sci. 2000; 97:2017. [PubMed: 10681441]
- (34). Gao J. Cur. Opinion Struct. Biol. 2003; 13:184.
- (35). Lill SON, Gao J, Waldrop GL. J. Phys. Chem. B. 2008; 112:3149. [PubMed: 18271571]
- (36). Sicinska D, Truhlar DG, Paneth P. J. Am. Chem. Soc. 2005; 127:5414. [PubMed: 15826179]
- (37). MacKerell AD Jr. Bashford D, Bellott M, Dunbrack RL, Evanseck JD, Field MJ, Fischer S, Gao J, Guo H, Ha S, Joseph-McCarthy D, Kuchnir L, Kuczera K, Lau FTK, Mattos C, Michnick S, Ngo T, Nguyen DT, Prodhom B, Reiher WE III, Roux B, Schlenkrich M, Smith JC, Stote R, Straub J, Watanabe M, Wiorkiewicz-Kuczera J, Yin D, Karplus M. J. Phys. Chem. B. 1998; 102:3586.
- (38). Jorgensen WL, Chandrasekhar J, Madura JD, Impey RW, Klein ML. J. Chem. Phys. 1983; 79:926.
- (39). Nam K, Gao J, York DM. J. Chem. Theory Comput. 2005; 1:2.
- (40). Kumar S, Bouzida D, Swendsen RH, Kollman PA, Rosenberg JM. J. Comput. Chem. 1992; 13:1011
- (41). Major DT, York DM, Gao J. J. Am. Chem. Soc. 2005; 127:16374. [PubMed: 16305206]
- (42). Jang S, Voth GA. J. Chem. Phys. 2000; 112:8747.
- (43). Schwieters CD, Voth GA. J. Chem. Phys. 1999; 111:2869.
- (44). Sprik M, Klein ML, Chandler D. Phys. Rev. B. 1985; 31:4234.
- (45). Hwang JK, Warshel A. J. Phys. Chem. 1993; 97:10053.
- (46). Pollock EL, Ceperley DM. Phys. Rev. B. 1984; 30:2555.
- (47). Chakrabarti N, Carrington T Jr. Roux B. Chem. Phys. Lett. 1998; 293:209.
- (48). Billeter SR, Webb SP, Agarwal PK, Iordanov T, Hammes-Schiffer S. J. Am. Chem. Soc. 2001; 123:11262. [PubMed: 11697969]
- (49). Kalyancker GD, Snell EE. Biochemistry. 1962; 1:594. [PubMed: 14453385]
- (50). Snider MJ, Wolfenden R. J. Am. Chem. Soc. 2000; 122:11507.
- (51). O'Leary MH. Acc. Chem. Res. 1988; 21:450.
- (52). Swanson T, Brooks HB, Osterman AL, O'Leary MH, Phillips MA. Biochemistry. 1998; 37:14943. [PubMed: 9778371]
- (53). Pauling, LC. The Nature of the Chemical Bond. Cornell University Press; Ithaca, NY: 1960.

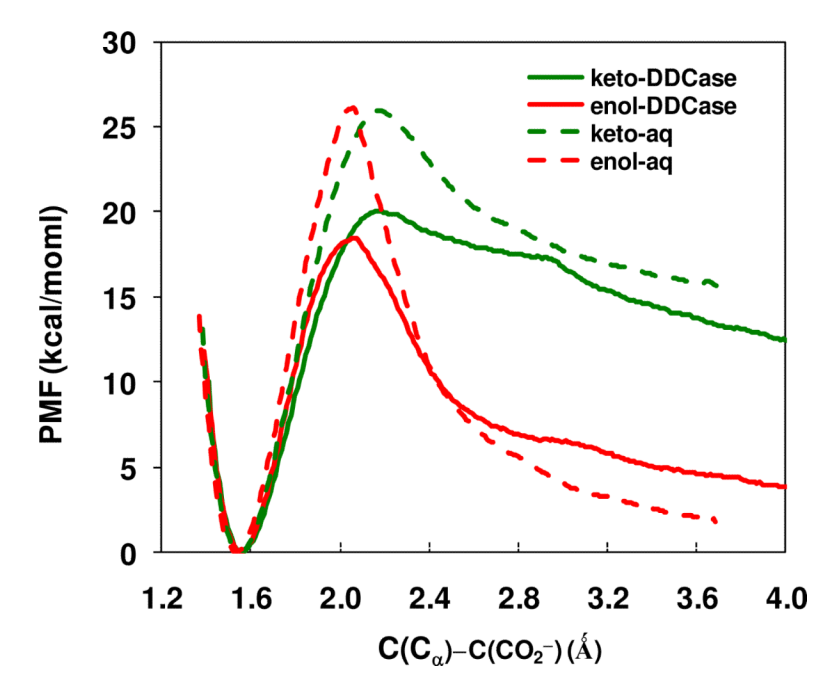


**Figure 1.**Computed potentials of mean force for the enzyme-catalyzed (solid) and uncatalyzed (dashed) decarboxylation of the PLP-dopa external aldimine in the N-protonated (keto) configuration in green and O-protonated (enol) tautomer in red.

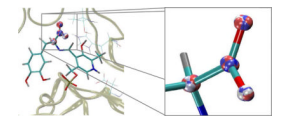


Figure 2.

#### Scheme 1.

Schematic illustration of the intramolecular proton transfer between the zwitterionic N-protonated Schiff base and the neutral O-protonated hydroxyimine of the PLP-dopa external aldimine cofactor in the decarboxylation reaction by dopa decarboxylase.

**Scheme 2.** Division between the QM (blue) and MM (black) region in the PLP-dopa external aldimine cofactor. The boundary atom is located at the C5A carbon.

### Table 1

Computed kinetic isotope effects and selected geometrical parameters at the transition state. Bond distances are given in angstroms, and angles are in degrees. Standard errors  $(\pm 1\sigma)$  in computed kinetic isotope effects are determined over ten separated block averages. Each KIE is obtained by using all data sampled in the PI-FEP/UM simulations.

	Dopa decarboxylase		Aqueous solution	
	O-protonated	N-protonated	O-protonated	N-protonated
<sup>12</sup> k/ <sup>13</sup> k (C)	$1.053 \pm 0.002$	$1.047 \pm 0.003$	$1.053 \pm 0.003$	$1.049 \pm 0.002$
$^{12}k/^{13}k(C_{\alpha})$	$1.037 \pm 0.006$	$1.026 \pm 0.005$	$1.030 \pm 0.003$	$1.034 \pm 0.003$
$^{1}k/^{2}k$ (H <sub><math>\alpha</math></sub> )	$1.053 \pm 0.032$	$1.144 \pm 0.066$	$0.975 \pm 0.051$	$1.137 \pm 0.051$
$Rc(C_{\alpha}$ -C)	2.07	2.17	2.06	2.17
$R(C_{\alpha} = N)$	1.36	1.39	1.34	1.38
$\theta(O = C = O)$	148.6	153.8	150.5	153.2